Extremal control for photovoltaic panels

Crina-Loredana Torous, Dumitru Popescu, Severus-Constantin Olteanu,
University 'Politehnica' of Bucharest
Faculty of Automatic Control and Computers
Bucharest, Romania, crina_torous@yahoo.com,
severus.olteanu@gmail.com

Chloé Lourdais
Ecole Centrale de Lille
Villeneuve D'Ascq, Lille, France
chloe.lourdais@gmail.com

***Abstract*— In this paper a methodology for extremal control of photovoltaic panels has been designed through the use of an embedded polynomial controller using robust approaches and algorithms. Also, a framework for testing solar trackers in a hardware in the loop (HIL) configuration has been established. Efficient gradient based optimization methods were put in place in order to determine the parameters of the employed photovoltaic panel, as well as for computing the Maximum Power Point (MPP). Further a numerical RST controller has been computed in order to allow the panel to follow the movement of the sun to obtain a maximum energetic efficiency. A robustness analysis and correction procedure has been done on the RST polynomial algorithm. The hardware in the loop configuration allows for the development of a test and development platform which can be used for bringing improvements to the current design and also test different control approaches. For this, a microcontroller based solution was chosen. The achieved performances of the closed loop photovoltaic panel (PP) system are validated in simulation using the MATLAB / SIMULINK environment and the WinPim & WinReg dedicated software. As it will be seen further in this paper, the extremal control of this design resides in a sequential set of computations used for obtaining the new Maximum Power Point at each change in the system.**

Keywords*— photovoltaic tracker; automatic control; HIL simulation; polynomial controller

I. INTRODUCTION

Renewable energy sources have been considered a viable solution for developing an environment friendly energy production infrastructure. Photovoltaic panels are an important source of renewable energy [1]. Because of the low efficiency of a photovoltaic cell, numerous optimization techniques have been implemented, in the scientific community, in order to improve it. Many papers act only upon the DC/DC converter as for example [11], whereas others treat the solar tracking problem [12]. Our solution is to use an optimal algorithm for computing the Maximum Power Point and to design a robust RST controller which controls the rotation of the photovoltaic panel in order to follow the sun's movement.

The rotation of the panel towards the sun can be done on two axes. In this paper the movement of the panel on a horizontal axis is considered fixed, thus reducing the risk for mechanical failure. Usually the sun is visible on an 180^0 domain over one day. A fixed solar panel has access to only 75^0 out of this domain, the losses being at sunrise and sunset. Allowing the panel to rotate in order to face the sun's rays directly brings significant improvement in energy harvesting. As a comparison, statistical data shows that the performance difference between a two axis orientated panel and a one axis oriented panel is around 4%, while the difference between a fixed panel and a one axis oriented panel varies around 24-32%. Another significant factor in choosing the number of axis on which to rotate the photovoltaic panel is also the cost. The one axis oriented photovoltaic panel configuration offers a good cost-performance ratio. The photovoltaic panel used in this article is a 30W photovoltaic panel: Ameresco Solar 30J.

The "Hardware in the loop" (HIL) validation has notable advantages when it comes to designing embedded controllers. Tests can be easily run in order to determine the stability, operation and fault tolerance of large scale systems, as it is the case, for energy networks. This paper will make use of an Arduino board in order to implement this structure. The microcontroller will hold the algorithms of the system controller. The extremal control in this paper, consists in computing in real time, the Maximum Power Point using optimal algorithms, such as the gradient Cauchy method and using a robust RST controller to rotate the panel to face the sun directly.

II. PHOTOVOLTAIC CONFIGURATION

A. Panel model

The functioning of a PN junction allows achieving an equivalent circuit model of a photovoltaic cell called the ideal model. This model is a current source connected in parallel to a diode. This is the simplest model to represent a photovoltaic cell; it has the advantage of having a reduced number of parameters (three parameters) required for the simulation of the characteristic curves I-V and P-V. However, it exhibits serious deficiencies when subjected to temperature and irradiance variations. An improvement of this model is done by the inclusion of one series resistance R_s and one shunt resistance R_{sh}. Thus, a new model is obtained, called "one diode model", being the most popular approach: it has a low number of unknown parameters (five parameters) and is more accurate than the ideal model, especially because it takes account of the change in the environment with a higher precision. On the other hand, an even more accurate model, which will be used in this article, is the two diodes one, shown in figure 1, presented in [4], [10].

978-1-5090-2720-0/16/$31.00 ©2016 IEEE

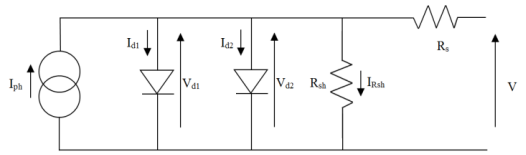

Fig. 1. Photovoltaic cell – Two diodes model

The output current of the photovoltaic cell can be written as:

$$I = I_{ph} - I_{01}\left[\exp\left(\frac{V+IR_s}{a_1V_T}\right)-1\right] - I_{02}\left[\exp\left(\frac{V+IR_s}{a_2V_T}\right)-1\right] - \frac{V+IR_s}{R_{sh}} \quad (1),$$

where:

I_{ph}	photovoltaic current	
I_{01} , I_{02}	saturation currents of the diodes	
R_s	series resistance	
R_{sh}	shunt resistance	
q	electron charge constant	$1.602 \cdot 10^{-19}$ C
a_1, a_2	shape factors	1 for ideal cell
N_s	number of cells wired in series	53
k	Boltzmann constant	$1.381 \cdot 10^{-23}$ J/K
T	cell temperature [K]	
V_T	Thermodynamic potential	$N_s \cdot k_b \cdot T/q$
I	Output current of the PV cell	
V	Output voltage of the PV cell	

Several parallel and series cells compose a photovoltaic module. N_{sh} (generally N_{sh}=1) gives the number of cells connected in parallel and Ns the number of series cells (Ns varies between 34 and 56 cells). In cases where N_{sh}=1, the characteristic equation (1) is the same but the thermodynamic potential V_T depends on N_s [3].

B. Photovoltaic characteristics

Equation (1) is an implicit equation where there are seven unknown parameters: I_{ph}, I_{01}, I_{02}, a_1, a_2, R_s and R_{sh} that are to be determined. Once they are identified, the model will allow us to compute the I-V and P-V characteristic curves. Indeed, each photovoltaic module has specific characteristics given by the datasheet information provided by the manufacturer, seen in the following table:

T_{STC}	Temp. at standard test condition	25 °C
G_{STC}	Iradiance at standard test cond	1000 W/m^2
V_{OC_STC}	Open circuit voltage	22.1 V
I_{SC_STC}	Short circuit currrent	1.74 A
V_{mp_STC}	Voltage at P_{mp_STC}	17.9 V
I_{mp_STC}	Current at P_{mp_STC}	1.68 A
K_i	Temp. coefficient of I_{SC_STC}	0.105 %/°C
K_V	Temp. coefficient of V_{OC_STC}	-0.360 %/°C
N_s	number of cells wired in series	36

The value of the current generated by the incidence of light I_{ph} can be computed as in (2), showing its dependence on temperature.

$$I_{ph} = \left(I_{ph\_STC} + K_i\Delta T\right)\frac{G}{G_{STC}} \quad (2),$$

where G is the surface irradiance of the cell and $\Delta T = T_{STC} - T$ is the difference between the external temperature and the temperature at Standard Test Conditions.

First, the two diodes saturation currents' equation, which considers the temperature variation, is given by:

$$I_{01} = I_{02} = \frac{I_{SC\_STC} + K_i\Delta T}{\exp\left(\frac{V_{oc\_STC} + K_v\Delta T}{\left(a_1 + a_2/p\right)V_T}\right) - 1} \quad (3)$$

Diode ideality factors a_1 and a_2 represent, respectively, the diffusion and recombination current components. Several researchers show that the diffusion current a_1 must be equal to 1 and the value of a_2 depends on the photovoltaic panel. It is found by experimentation that the best match between the proposed model and practical I-V curve is observed when $(a_1+a_2)/p=1$ and $p \geq 2{,}2$. Here, we have found that the best value of a_1 and a_2 are respectively 1 and 1.2. To conclude, the expression for the diode saturation current of the two diodes I_{01} and I_{02} is:

$$I_{01} = I_{02} = \frac{I_{SC\_STC} + K_i\Delta T}{\exp\left(\frac{V_{oc\_STC} + K_v\Delta T}{V_T}\right) - 1} \quad (4)$$

The series resistance, in the figure 1, called R_s, models the resistance contained in the semiconductor and the shunt resistance, named R_{sh} in the figure, models the current leakage through a resistive branch which is parallel to the generator and to the two diodes. These losses are less important than those represented by the resistance R_s; so the value of the resistance R_s is very low compared to the value of R_{sh}. The values of the resistors R_s and R_{sh} are obtained by iteration and calculated simultaneously. According to the characteristic equation (1), at Maximum Power Point, R_{sh} can be expressed in terms of R_s as follows:

$$R_{sh} = \frac{V_{mp\_STC} + I_{mp\_STC}\cdot R_s}{I_{ph} - I_{01}\left[\exp\left(\frac{V_{mp\_STC} + I_{mp\_STC}\cdot R_s}{a_1V_T}\right)-1\right] - I_{02}\left[\exp\left(\frac{V_{mp\_STC} + I_{mp\_STC}\cdot R_s}{a_2V_T}\right)-1\right] - \frac{P_{mp\_E}}{V_{mp\_STC}}} \quad (5)$$

The voltage V_{mp_STC}, the current I_{mp_STC}, and the power P_{mp_STC} are at maximum power point, and found in the manufacturer datasheets. The idea of the following algorithm is, by iteratively increasing the value of R_s while simultaneously calculating the R_{sh} value, to compare the value of the calculated maximum power point P_{mp_C}, with the value of experimental maximum power $P_{mp\_E}=P_{mp\_STC}$, given by the manufacturer's datasheets, in order to have the smallest difference.

In this paper we use Newton Raphson's method to solve the equation (6) and find the value of I ($0 \leqslant I \leqslant I_{SC\_STC}$) for different values of V ($0 \leqslant V \leqslant V_{OC\_STC}$):

$$f(I) = I - I_{ph} + I_{01}\left[\exp\left(\frac{V+IR_s}{a_1V_T}\right)-1\right] + I_{02}\left[\exp\left(\frac{V+IR_s}{a_2V_T}\right)-1\right] + \frac{V+IR_s}{R_p} = 0 \quad (6)$$

This method is described by the expression:

$$I_{n+1} = I_n - \frac{f(I_n)}{f'(I_n)} \tag{7}$$

With the set of data of I and V, it is possible to calculate de power P and the maximum power P_{mp_C} and apply the following algorithm:

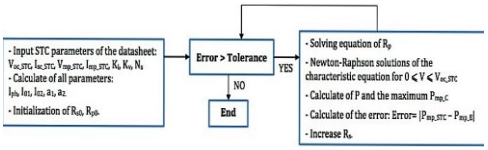

Fig. 2. Algorithm for the determination of R_s and R_p using the Newton-Raphson method

TABLE I. RESULTS OF PARAMETERS CALCULATION

$I_{01}=I_{02}$	I_{ph}	a_1	a_2	R_s	R_{sh}
$7.31.10^{-11}$ A	1.74 A	1	1,2	0.892 Ω	529.657 Ω

With these values of resistors R_s and R_{sh} and the simulation given by the characteristic equation (1) and the Newton-Raphson method, we find a voltage at maximum power point of V_{mp_C} = 17,89 V (V_{mp_STC} = 17,9 V) and a power at the maximum power point of P_{mp_C} = 28,9 W (P_{mp_STC} = 30 W). The model is confirmed as the results given by the simulations are close to the datasheets and then to the experimental values. These results allow plotting the characteristic curves I-V and P-V. In the figures that follow, it can be noticed that the model offers a good approximation of the real one.

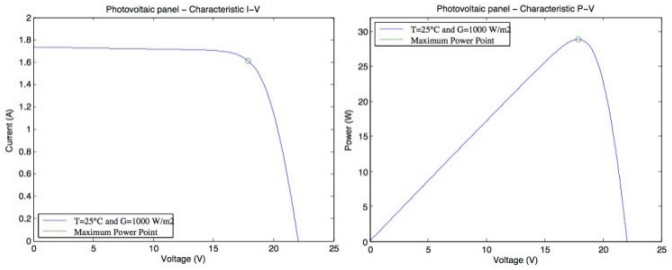

Fig. 3. Simulation of the characteristic I-V and P-V of the Ameresco Solar photovoltaic panel.
a. Characteristic I-V; **b.** Characteristic P-V.

III. EXTREMAL CONTROL

A. Maximum Power Point Tracking

The objective is to control the maximum power of a photovoltaic panel with a DC motor that allows the solar panel to follow the direction of sunlight.

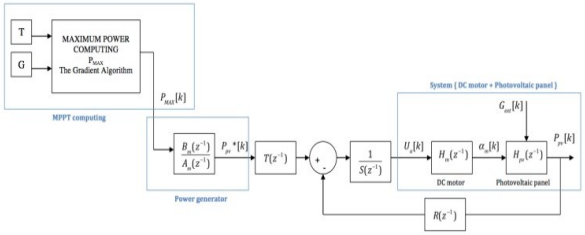

Fig. 4. Diagram of the maximum power point tracking and control.

First, an algorithm computes the maximum power point, here we use the gradient algorithm. Secondly, an RST regulator controls the system composed of a DC motor and the photovoltaic panel in order for the system to function at the power imposed by the reference power.

In order to benefit from the maximum power of a photovoltaic panel an MPPT control algorithm will be used. In this application, we have chosen the gradient algorithm for its robustness and high speed of convergence, as well as its simplicity in being implemented on an embedded controller. The parameters are: the starting point (I_0, V_0), the direction λ and the precisions ε_1, ε_2. The next step involves evaluating the gradient of the function (1) squared for each point V. The algorithm stops when the gradient becomes too small compared to the precision, which means that at the point in time k, we have identified the solution for equation (6) that can be used to find the maximum power point [2].

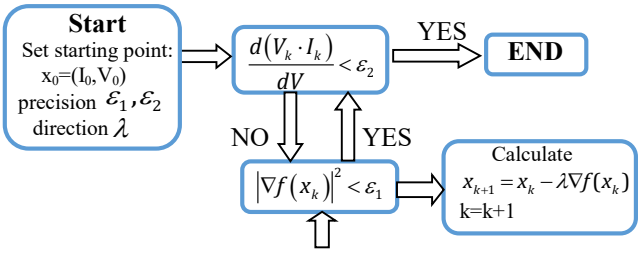

TABLE II. RESULTS OBTAINED BY THE GRADIENT ALGORITHM FOR COMPUTING THE MAXIMUM POWER POINT

I_0	V_0	ε	λ_0	V_{mp}	I_{mp}	$P_{mp}=I_{mp}\cdot V_{mp}$
0.5A	0.4V	0.0001	0.5	31.25V	0.62A	19.32W

B. The photovoltaic panel and motor dynamics models

The complete system consists of photovoltaic modules, an electric DC motor, a sensor for measuring the voltage and the current at the terminal of the PV panel.

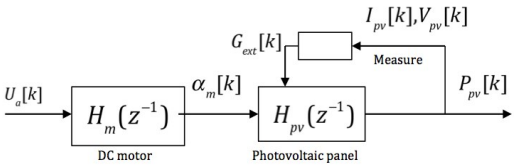

Fig. 5. Block diagram of the system{ DC motor + the photovoltaic panel }

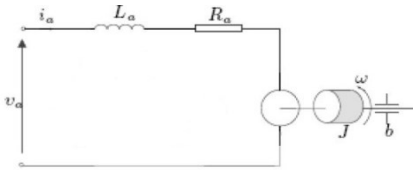

Fig. 6. Schematic block diagram of the DC motor

Through the equivalent electro-mechanical model in Fig.6, the dynamic of the DC motor may be expressed by the following equations [6]. The first one comes from the Kirchhoff laws and the second one from the angular momentum theorem:

$$u_a(t) = u_{R_a}(t) + u_{L_a}(t) + e_a(t) = R_a.i_a(t) + L_a.\frac{di_a(t)}{dt} + e_a \tag{8}$$

$$J.\frac{d\omega(t)}{dt} = C_m(t) + C_b(t) = K_c.i_a(t) - b.\omega(t) \quad (9)$$

TABLE III. MOTOR PARAMETERS

U_a	Armature voltage	V
I_a	Armature current	A
ω_m	Speed of the rotor	rad.s^{-1}
R_a	Motor resistance	1,45Ω
L_a	Motor inductance	15,5. 10^{-3} H
J	Motor inertia	0,48kg.m^2
$e_a(t)=K_e.\omega_m(t)$	Motor's Back EMF	V
$C_m(t)=K_c.i_a(t)$	Motor torque	N.m
$C_b(t)=-b.\omega_m(t)$	Friction torque	N.m
K_c	Motor torque constant	0,1 N.m.A^{-1}
K_e	Motor voltage constant	0,1V.rad^{-1}.s
b	Friction coefficient	0,2N.m.s

The relation between the panel positioning angle and the speed of the rotor is:

$$\Omega(s) = s \cdot \alpha_m(s) \quad (10)$$

By using the Laplace Transforms, the above equations can be expressed in terms of s.

$$H_m(s) = \frac{\alpha_m(s)}{U_a(s)} = \frac{1}{s}.\frac{K_e}{(L_aJ).s^2 + (R_aJ + L_ab).s + (R_ab + K_e^{\,2})} \quad (11)$$

The power on a photovoltaic module depends not only on the power contained in the sunlight, but also on the angle between the module and the ray of sunlight. When the surface of the panel and the sunlight are perpendicular to each other, the photovoltaic module works at the maximum power point. Indeed, rays of sunlight with an angle of incidence 90° tend to be absorbed, while lower angles tend to be reflected. The solar radiation absorbed by the photovoltaic module (G_m) is the component of the incident solar radiation (G_{ext}), which is perpendicular to the module surface [5]. The angle of incidence (α_m) is the angle between the tilted module surface and the external ray of sunlight. Consequently, the expression between these parameters is:

$$G_m = G_{ext}.\sin(\alpha_m) \quad (12)$$

The role of the motor is to make the photovoltaic panel follow the solar radiation. Consequently, the angle α_m stays very small and we can approximate the function "sinus" around the value of zero, see equation (13). We suppose that this approximation is correct for $-15° \leq \alpha_m \leq 15°$. For the start of the experience, we consider that we launch the panel approximately perpendicular of the sunlight because we can know the relative position of the sunlight.

$$G_m = G_{ext}.\alpha_m \quad (13)$$

Thus, the power delivered by a solar panel positioned at irradiation G_{ext}, which has a component perpendicular to the panel, called G_m, is equal to the maximum power that it could deliver if it was placed at irradiation G_m: $P_{pv\_Gext}=P_{pv\_MAX\_Gm}$.

Besides, the power at maximum power point can be written as the multiplication of the current I_{mp_STC} and the voltage V_{mp_STC}. By using the characteristic equation (1) at the maximum power point: $I= I_{mp\_STC}$ and $V=V_{mp\_STC}$, only the term I_{ph} depends on the radiation G thus we have:

$$\frac{dP_{pv\_MAX}}{dG_m} = V_{mp\_STC}.\frac{1}{G_{STC}}.\left(K_i\Delta T + I_{sc\_STC}\right) = K_{pv} \quad (14)$$

The value of K_i is very small and we can neglect the term in K_i, so the derivation of the power at the maximum power point P_{pv_MAX}, compared with the irradiance G_m is a constant term and the power at maximum point and the external radiation are proportional.

$$P_{pv\_G_{ext}} = P_{pv\_MAX\_G_m} = K_{pv}.G_m = K_{pv}.G_{ext}.\alpha_m \quad (15)$$

To conclude, by using this equation, the transfer function of the solar panel is:

$$H_{pv}(s) = \frac{P_{pv}(s)}{\alpha_m(s)} = K_{pv}.G_{ext} \quad (16)$$

By using a voltmeter and an ammeter to measure the terminal voltage and the current of the photovoltaic panel, it is possible to determine the value of the external radiation with the following formula, determined by (1) and (2):

$$G_{ext} = \frac{G_{STC}}{I_{sc\_STC}}.\left[I_{pv} + I_{01}.\left(\exp\left(\frac{V_{pv} + I_{pv}R_s}{a_1V_T}\right)\right) + I_{02}.\left(\exp\left(\frac{V_{pv} + I_{pv}R_s}{a_2V_T}\right)\right) + \frac{V_{pv} + I_{pv}R_s}{R_p}\right] \quad (17)$$

The transfer function of the photovoltaic and motor system becomes:

$$H(s) = K_{pv}.G_{ext}\frac{K_m}{a_ms^3 + b_ms^2 + c_ms} \quad (18)$$

Where the parameters a_1, a_2, a_3, b_1, b_2 and b_3 depend only on the parameters of the DC motor, as follows:

$$\begin{aligned} a_{\mathrm{m}} &= L_a * J \\ b_{\mathrm{m}} &= R_{\mathrm{a}} * J + L_{\mathrm{a}} * \mathrm{b} \\ c_{\mathrm{m}} R_{\mathrm{a}} &* \mathrm{b} + K_e^2 \end{aligned} \quad (19)$$

The calculus led to:

$$H(s) = K_{pv} \cdot G_{ext} \cdot \frac{0.1}{s^3 7440.10^{-3} + s^2 6991.10^{-1} + s3.10^{-1}} \quad (20)$$

C. RST controller design

By discretizing the continuous model of the system with a zero-order hold discretization and a sampling period $T_r = 0.05$s, we have obtained the discrete model, as follows:

$$H(z^{-1}) = \frac{B(z^{-1})}{A(z^{-1})} = K_{pv}.G_{ext}.\frac{B'(z^{-1})}{A'(z^{-1})} \quad (21)$$

Where the function $B'(z^{-1})/A'(z^{-1})$ represent the discrete model of the DC motor. The numerical application gives:

$$\begin{cases} A'(z^{-1}) = 1 - 1.988 \cdot z^{-1} + 0.9971 \cdot z^{-2} + 0.009111 \cdot z^{-3} \\ B'(z^{-1}) = 1.183 \cdot 10^{-4} \cdot z^{-1} + 2.201 \cdot 10^{-4} \cdot z^{-2} + 1.364 \cdot 10^{-5} \cdot z^{-3} \end{cases} \quad (22)$$

The variation of the irradiance G_{ext} is low compared to the dynamics of the DC motor, as such only the motor imposes the dominant dynamics of the system and we consider that the term $G_{ext} \cdot K_{pv}$ is a multiplicative constant included after computing the regulator. We can conduct the analysis on polynomials $A'(z^{-1})$ and $B'(z^{-1})$.

For computing the A_m and B_m polynomials for the power generator, we need to impose the pair (ζ_n, ω_{0n}) in order to follow the tracking performances desired. We have imposed $\zeta_n = 0{,}8$ and $\omega_{0n} = 10$ rad.s^{-1}. By discretization, we have obtained:

$$\frac{B_m(z^{-1})}{A_m(z^{-1})} = \frac{0.095495 \cdot z^{-1} + 0.073072 \cdot z^{-2}}{1 - 1.280762 \cdot z^{-1} + 0.449329 \cdot z^{-2}} \quad (23)$$

For the discrete model $A'(z^{-1})/B'(z^{-1})$, an RST controller was designed to achieve wanted performances in tracking and regulation. Controller polynomials $R(z^{-1})$ and $S(z^{-1})$ determine the regulation performances and the polynomial T(z-1) involves the performance in tracking [7]. The sample time is also of 0.05 seconds.

The desired poles introduced by the polynomial $P(z^{-1})$, which is the characteristic polynomial of the system, specify the performance of the closed loop system [8].

$$P(z^{-1}) = A'(z^{-1}) \cdot S'(z^{-1}) + B'(z^{-1}) \cdot R'(z^{-1}) \quad (24)$$

We desire a response of a second order form for the polynomial P and we have allocated the dominant poles given by $\zeta = 0{,}87$ and $\omega_0 = 5$ rad.s^{-1}. By discretization we can determine the characteristic polynomial $P(z^{-1})$:

$$P(z^{-1}) = 1 - 1.596847 \cdot z^{-1} + 0.647265 \cdot z^{-2} \quad (25)$$

As a result, the calculation of controller parameters $R'(z^{-1})$ and $S'(z^{-1})$ involves the resolution of the Bezout equation represented by (23), and $T'(z^{-1})$ must be chosen to ensure a static gain between P_{pv}*[k] and P_{pv}[k] (notations form Fig.10):

$$T(z^{-1}) = \begin{cases} G = \dfrac{1}{B(1)}, B(1) \neq 0 \\ G = 1 \end{cases} \cdot P(z^{-1}) \quad (26)$$

In order to improve the command, to eliminate the stationary error and augment the tolerance to uncertainties and perturbations, auxiliary poles are added.

The polynomial S receives another simple pole (a-z^{-1}) in order to eliminate the stationary error. Another pole with multiplicity of 2, ($1+z^{-1}$) is added to the R polynomial to increase the damping of high frequencies. Finally, a band-stop filter is added (Notch filter) to the Sensitivity function S_{py}. This is chosen to filter out frequencies that experimentally were identified to affect the system. Its form is shown in article [13], represented as:

$$F_{notch}(z^{-1}) = K \frac{1 - 2 \cdot \cos(\omega) \cdot z^{-1} + z^{-2}}{1 - 2 \cdot r \cdot \cos(\omega) \cdot z^{-1} + r^2 \cdot z^{-2}} \quad (27)$$

where ω is the central stop frequency, and r is a value between 0.9 and 0.99, giving the bandwidth.

As such, choosing r=0.9 and a frequency of 0.15, one gets the added polynomials: in S, $1 - 1.756z^{-1} + z^{-2}$, and in P, $1 - 1.058z^{-1} + 0.81z^{-2}$. The robustness can be seen in the spectrum of the sensitivity transfer function:

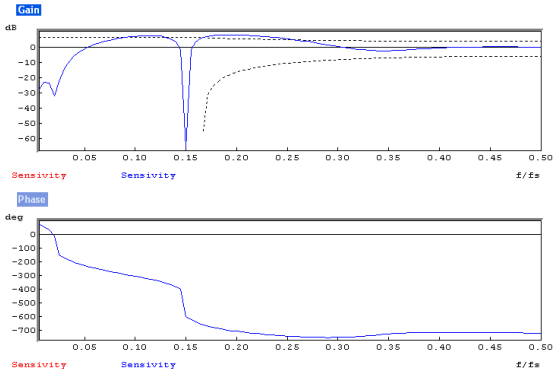

Fig. 7. Sensitivity function

The resolution of the R,S,T polynomials is done in the specialized software Winreg. For the complete system DC motor and photovoltaic panel, the polynomials R, S and T depend on the polynomials R', S' and T' and expressions are:

$$R(z^{-1}) = \frac{1}{K_{pv} G_{ext}} R'(z^{-1}), \quad S(z^{-1}) = S'(z^{-1}), \quad T(z^{-1}) = \frac{1}{K_{pv} G_{ext}} T'(z^{-1}) \quad (28)$$

The following Matlab-Simulink diagram block (see Fig. 8) represents the maximum power point tracking element (the gradient algorithm) and the control of the system by the previous RST controller, and figure Fig. 9 shows the response of the complete system. We have inserted a step disturbance at T = 6 sec, in order to observe the regulation performance. The RST controller achieves performances in tracking and regulation.

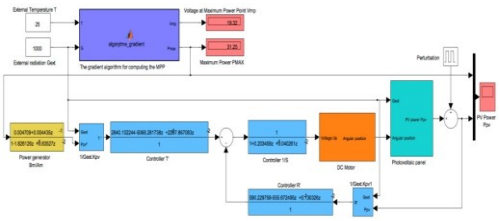

Fig. 8. Simulink diagram of the maximum power point tracking and the control of the motor and the photovoltaic panel by a RST controller

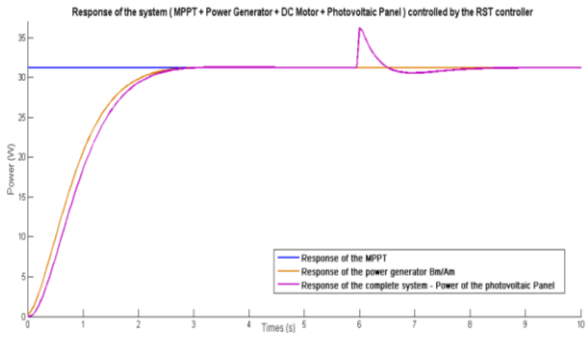

Fig. 9 .Response of the system motor and the photovoltaic panel controlled by the RST controller.

D. Hardware In the Loop validation

Next we will present our HIL testing procedure with implementation on an Arduino Uno microcontroller. The objective of this part to implement the previous RST controller in a microcontroller in order to control the system (DC motor + Photovoltaic panel). We have used an Arduino Uno, connected on serial port with Simulink. The diagram block is:

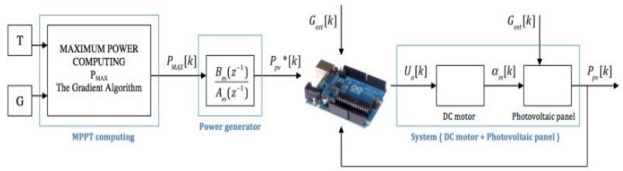

Fig.10. Diagram of the maximum power point tracking and control of the system { DC motor + Photovoltaic panel }by an Arduino Uno

By implementing the RST control in the Arduino, we have modified the last Simulink simulation such that the block connected to the external device (Packet Output and Packet Input) replaces the blocks concerning the RST controller [9]. The sample time is always of 0.05 seconds. We have implemented the following formulas in the Arduino:

$$\begin{cases} \varepsilon[k] = \dfrac{1}{G_{ext}.K_{pv}}\left(t_0.P_{pv}^*[k] + t_1.P_{pv}^*[k-1] + t_2.P_{pv}^*[k-2]\right) \\ \qquad - \dfrac{1}{G_{ext}.K_{pv}}\left(r_0.P_{pv}[k] + r_1.P_{pv}[k-1] + r_2.P_{pv}[k-2]\right) \\ U_a[k] = \varepsilon[k] - s_1.U_a[k-1] - s_2.U_a[k-2] \end{cases} \quad (29)$$

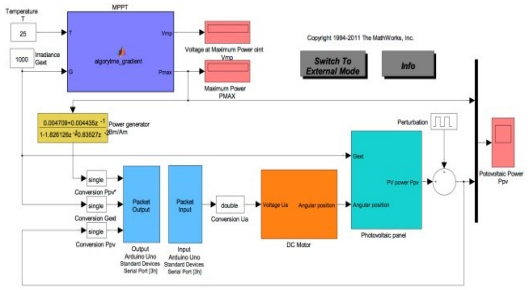

Fig.11. Simulink diagram of the complete system (MPPT + Power generator + DC Motor + Photovoltaic Panel) controlled by the Arduino Uno

In order to observe the regulation performance, we have inserted a step disturbance at T = 6 sec and we can observe that the imposed performances in tracking and in regulation are respected by the system.

Furthermore, we can note that there is a delay of 0.5 seconds specific for the Arduino Uno initial startup time.

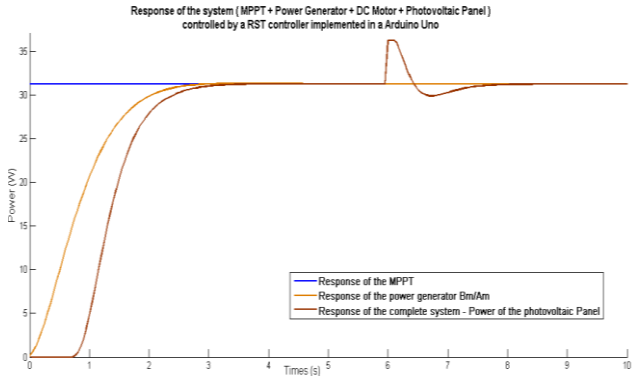

Fig. 6. Results of the Simulink simulation of the complete system (MPPT + Power generator + DC Motor + Photovoltaic Panel) controlled by the Arduino Uno

IV. CONCLUSION

The paper showed the results obtained in modelling a photovoltaic panel using a two diode model, simulated the panel characteristics and designed an RST controller to position the panel in an optimal position towards the sun. The gradient algorithm has managed to attain the MPP in an optimum number of steps. The RST controller presented good performances in tracking and regulation and it has been simulated on an Arduino Uno platform. The HIL (Hardware in the Loop) validation approach can be reiterated for any PV panel and method. A physical implementation of the system will be a good confirmation or this design and validation procedure.

REFERENCES

[1] T. Salmi, M. Bouzguenda, A. Gastli, A. Masmoudi, MATLAB/Simulink Based Modelling of Solar Photovoltaic Cell, International Journal Of Renewable Energy Research, Vol.2, No.2, 2012.

[2] P. Borne, D. Popescu, F. Gh Filip, D. Ştefănoiu, Optimization in Enginerring Sciences Exact Methods, Wiley, 2013.

[3] M. Azzouzi, L. Mazzouz and D. Popescu Matlab-Simulink of Photovoltaic System Based on a Two-Diode Model, Proceedings of the World Congress on Engineering 2014 Vol I, WCE 2014, London.

[4] D. Bonkoungou, Z. Koalag, D. Njomo, Modelling and Simulation of photovoltaic module considering single-diode equivalent circuit model in MATLAB, International Journal of Emerging Technology and Advanced Engineering, Volume 3, Issue 3, March 2013.

[5] R. Hernanz, C. Martín, Z. Belver, L. Lesaka, Z. Guerrero, Modelling of Photovoltaic Module, International Conference on Renewable Energies and Power Quality,(ICREPQ'10), Granada (Spain), 2010.

[6] T. Tudorache ,L. Kreindler, Design of a Solar Tracker System for PV Power Plants, Acta Polytechnica Hungarica Vol. 7, No. 1, 2010.

[7] I.D. Landau, G. Zito, Digital Control Systems, Springer, 2006.

[8] D. Popescu, D. Stefanoiu, C. Lupu, C. Petrescu, B. Ciubotaru, C. Dimon, Automatica Industriala, AGIR, 2006.

[9] https://www.arduino.cc/en/Guide/HomePage.

[10] C. Miron, D. Popescu, A. Atouche, N. Christov, Observer based control for a PV system modeled by a Fuzzy Takagi Sugeno model, System Theory, Control and Computing (ICSTCC), 2015 19th International Conference on, Cheile Gradistei, pp. 652-657, 2015.

[11] M. A. Enany, M. A. Farahat, Ahmed Nasr, Modeling and evaluation of main maximum power point tracking algorithms for photovoltaics systems, Renewable and Sustainable Energy Reviews, Volume 58, May 2016